

# Transmission electron microscopy and cathodoluminescence of tensile-strained $\text{Ga}_x\text{In}_{1-x}\text{P}/\text{InP}$ heterostructures. II. On the origin of luminescence heterogeneities in tensile stress relaxed $\text{Ga}_x\text{In}_{1-x}\text{P}/\text{InP}$ heterostructures

F. Cléton and B. Sieber<sup>a)</sup>

Laboratoire de Structure et Propriétés de l'Etat Solide, URA CNRS 234, Bâtiment C6, Université des Sciences et Technologies de Lille, 59655 Villeneuve d'Ascq Cedex, France

A. Bensaada and R. A. Masut

Groupe de Recherche en Physique et Technologie des Couches Minces, Université de Montréal, C.P. 6218, Montréal, Québec H3C 3A7, Canada

J. M. Bonard and J. D. Ganière

IMO, Département de Physique, Ecole Polytechnique Fédérale de Lausanne, CH 1015 Lausanne, Switzerland

(Received 17 January 1996, accepted in publication 18 April 1996)

We have determined the origin of the spatial luminescence fluctuations observed between the dark line defects present in tensile strained  $\text{Ga}_x\text{In}_{1-x}\text{P}/\text{InP}/n^+-\text{InP}$  heterostructures (Part I [F. Cléton *et al.* *J. Appl. Phys.* **80**, 827 (1996)]). For that purpose, we have undertaken semi-quantitative and spectroscopic cathodoluminescence (CL) measurements on various specimens in areas exhibiting CL contrasts which could be as large as 80%. The analysis of the variation of the CL polychromatic signal with electron beam energy allowed us to get information on the diffusion-recombination (DR) parameters of the areas under study. From the correlation between the local relaxation level of these areas and their DR parameters, we can conclude that the variation of the misfit dislocations density at the  $\text{Ga}_x\text{In}_{1-x}\text{P}/\text{InP}$  interface is at the origin of the luminescence heterogeneities. We also demonstrate that recycling, by the  $\text{Ga}_x\text{In}_{1-x}\text{P}$  epilayer, of the photons originating from the heavily doped InP substrate, enhances the CL contrast between areas exhibiting different relaxation levels.

© 1996 American Institute of Physics. [S0021-8979(96)09014-7]

## I. INTRODUCTION

It has been shown in Part I<sup>1</sup> that the microstructure of tensile stress relaxed (001)-oriented  $\text{Ga}_x\text{In}_{1-x}\text{P}/\text{InP}$  heterojunctions is made of (i) twins in the  $[1\bar{1}0]$  ( $\beta$ ) direction and stacking faults in the  $[110]$  ( $\alpha$ ) direction and (ii) networks of perfect misfit dislocations located between the twins and heterogeneously distributed within the interface. According to cathodoluminescence observations (CL), the twins and stacking faults, associated with their partial dislocations, are very efficient nonradiative centers since they are imaged as dark line defects (DLDs). The DLDs are separated one from each other by areas of various luminescence intensities. The CL contrast between the areas in one sample can be as large as 40%, and no structural defects could be seen by CL. Furthermore, 77-K CL spectroscopic measurements performed on these areas have shown that, with a few exceptions, their luminescence intensity decrease when the relaxation level increases. The aim of Part II of this paper is to decide between the different assumptions, made in Part I, on the origin of luminescence fluctuations in  $\text{Ga}_x\text{In}_{1-x}\text{P}/\text{InP}$  heterojunctions. The assumptions are (1) inhomogeneities of misfit dislocation and (2) variations, in the epilayer, of the doping level and/or the diffusion length. Since dislocations are known to act as efficient nonradiative recombination centers, it is reasonable to believe that assumption 1 induces spatial

variations of the interface recombination velocity. Therefore, an experiment was needed which allowed us to discriminate between interface recombination velocity fluctuations and doping level as well as diffusion length heterogeneities. For that purpose, we have chosen the accelerating beam energy  $E_0$  dependence of the spectroscopic and semi-quantitative polychromatic CL signals, since these two experiments have already shown to be suitable for the determination of the diffusion-recombination (DR) parameters in homojunctions.<sup>2</sup>

The  $n\text{-Ga}_x\text{In}_{1-x}\text{P}/n\text{-InP}/n^+-\text{InP}$  heterojunctions studied are similar, with respect to the epilayer to substrate doping level ratio, to an  $n\text{-InP}/n^+-\text{InP}$  homojunction we have studied in detail previously by spectroscopic and quantitative CL analysis (see Ref. 2). Both of them have been grown by MOCVD in the same reactor. The InP/InP sample consisted of an epilayer doped by residual impurities to a level of about  $3 \times 10^{14} \text{ cm}^{-3}$ , and a substrate highly doped at  $1.7 \times 10^{19} \text{ cm}^{-3}$ . In that structure, the epilayer CL was found to be produced, not directly by the electron beam excitation, but indirectly by the recycling of the photons emitted by the substrate under electron beam illumination. The polychromatic semi-quantitative CL experimental results [ $I_{\text{CL}} = f(E_0)$  curves] obtained at 300 K were fitted by theoretical curves calculated with a model based on the excess minority carriers diffusion in the structure.

The analysis of the CL results we present is based on those obtained on the InP/InP homojunction where the InP epilayer diffusion length and the interface recombination ve-

<sup>a)</sup>Electronic mail: Brigitte.Sieber@univ-lille1.fr

TABLE I. Main parameters of the  $\text{Ga}_x\text{In}_{1-x}\text{P}/\text{InP}/\text{InP}$  samples studied in the present work.  $x$  is the gallium composition of the epilayer,  $\Delta a/a$  is the lattice-mismatch determined from the gallium composition  $x$  and  $R$  is the strain relaxation as measured by HRXRD.

Heterojunction	$x_{\text{Ga}}$ (%)	$\Delta a/a$ (%)	$R[\bar{1}\bar{1}0]$ (%)	$R[110]$ (%)	Ga <sub>x</sub> In <sub>1-x</sub> P epilayer thickness	InP buffer layer thickness	Experiments
					$t_1$ ( $\mu\text{m}$ )	$t_2 - t_1$ (nm)	
CD 21S	5.5	0.39	4.6	7.3	1.12	100	SEM/CL imaging + spectroscopy
CF 88S	6.5	0.47	1.5	1.5	0.4	25	SEM/CL imaging + spectroscopy + TEM
CF 86S	7.8	0.56	3.6	12.9	0.4	25	SEM/CL imaging + spectroscopy
CE 84S	11.2	0.8	13	43	0.55	25	SEM/CL imaging + spectroscopy + TEM

locity were found equal to  $0.7 \mu\text{m}$  and  $4 \times 10^5 \text{ cm/s}$ , respectively.

## II. EXPERIMENTAL DETAILS

The  $\text{Ga}_x\text{In}_{1-x}\text{P}$  epilayers were grown at  $640^\circ\text{C}$  on (001)-oriented sulfur-doped ( $n \sim 1 \times 10^{19} \text{ cm}^{-3}$ ) InP substrates using a computer-controlled cold-wall horizontal low-pressure MOCVD reactor.<sup>3</sup> Prior to the  $\text{Ga}_x\text{In}_{1-x}\text{P}$  deposition, an InP buffer layer was grown directly on the preheated surface in order to improve the crystallographic quality of the  $\text{Ga}_x\text{In}_{1-x}\text{P}/\text{InP}$  interface. The nominally undoped  $\text{Ga}_x\text{In}_{1-x}\text{P}$  and InP epilayers had residual type  $n$  impurities ( $n = 3 \times 10^{14} \text{ cm}^{-3}$ ). High resolution x-ray diffraction (HRXRD) and low-temperature photoluminescence were used to determine the gallium composition in the epilayers and the amount of relaxation.

77 K CL spectra were made first on areas located between DLDs and exhibiting different luminescence intensities; they were selected by CL imaging. We have chosen to study preferentially samples with a low-mismatch ( $\Delta a/a < 0.6\%$ ; Table I) since, as shown in part I of the paper,<sup>1</sup> the areas separating the DLDs are much larger in low-mismatched samples, and are therefore more suitable for our experiments. Care had to be taken for the luminescence to be homogeneous over an area much wider than the lateral extension of the generation volume of the electron-hole pairs. The spectra were recorded on a Cambridge Stereoscan 360 fitted with an Oxford CL system and a Jobin-Yvon HR250 monochromator which allowed a spectral resolution of about 1 meV. In a few cases, room temperature CL spectra were recorded for various values of the accelerating beam energy  $E_0$ . Then, polychromatic CL intensity ( $I_{\text{CL}}$ ) was recorded on areas exhibiting different relaxation levels. This was done at room temperature as a function of accelerating beam energy  $E_0$ , on a Cambridge Stereoscan 250 equipped with an Oxford CL system. As it is noticed in Table I, two specimens

have been characterized previously by transmission electron microscopy (TEM). The nature and distribution of the structural defects present in a low and in a highly mismatched sample (CF 88S and CE 84S, respectively) have been presented in Part I of this paper.<sup>1</sup>

## III. BEAM ENERGY DEPENDENT SPECTROSCOPIC AND SEMI-QUANTITATIVE CL EXPERIMENTS ON A LOW-MISMATCHED SAMPLE

Since it is not possible to determine a diffusion length larger than the epilayer thickness<sup>4</sup> a low-mismatched sample (CD 21S, Table I) with a large epilayer thickness ( $t_1 = 1.1 \mu\text{m}$ ) was first chosen in order to determine the diffusion-recombination (DR) parameters in the structure by means of polychromatic semi-quantitative CL measurements [ $I_{\text{CL}} = f(E_0)$  curves]. In parallel, we have also studied the luminescence generation mechanism in this  $\text{Ga}_x\text{In}_{1-x}\text{P}/\text{InP}$  heterojunction by means of CL spectroscopic measurements. The results of such an investigation are presented first, since they are essential in the analysis of polychromatic  $I_{\text{CL}}$  curves.

The sample exhibited very high luminescence fluctuations such as that shown in Fig. 1. Therefore, bright (BA) and dark (DA) areas with a CL contrast as large as 80% at low accelerating beam energies (Table II) could be selected. Figure 2 shows CL spectra of the dark and bright areas. It can be seen in this figure that the CL peak associated with the dark area (Fig. 1) occurs at a higher energy than that associated with the bright area (Fig. 1). Therefore, these two areas were definitely selected on the basis of their spectroscopic 77-K CL spectra (Fig. 2). Since a decrease of the residual strain leads to an energetical increase (blueshift) of both the conduction band—light-hole valence band (CB-lh) and conduction band—heavy-hole valence band (CB-hh) transitions<sup>5</sup> of the  $\text{Ga}_x\text{In}_{1-x}\text{P}$  tensile stress epilayer (cf. Sec.

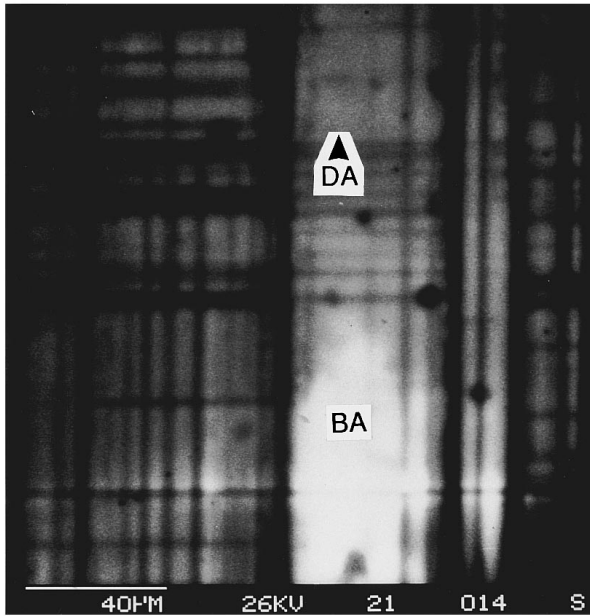


FIG. 1. Plan-view CL polychromatic image of CD 21S sample ( $x_{\text{Ga}}=5.5\%$ ;  $\Delta a/a=0.39$ ;  $R[1\bar{1}0]=4.6\%$ ;  $R[110]=7.3\%$ ). The areas labeled bright and dark exhibiting a very high contrast of 20% at 26 keV have been studied by semi-quantitative CL experiments.

TABLE II. CD 21S sample. Variation, with  $E_0$ , of the polychromatic CL intensity recorded at 300 K on the bright and dark areas. The CL contrast is the ratio of the intensities difference to the intensities sum.

$E_0$ (keV)	CL intensity (a.u.) bright area	CL intensity (a.u.) dark area	CL contrast (%)
2	1.05	0.100	82.61
5	3.8	0.33	84
10	6.9	0.49	86.7
15	8.5	0.72	84.4
20	24.7	6.2	59.9
26	66.3	43.6	20.6
30	103.5	85.3	28.6
36	165.2	159.2	18.5
40	180.2	176.4	1

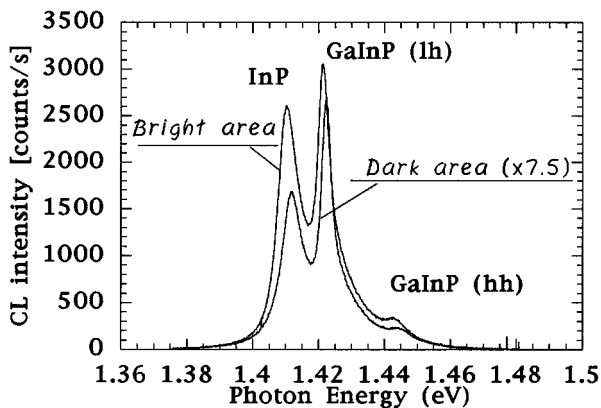


FIG. 2. 77-K CL spectra of the bright and dark areas shown in Fig. 1. Low-mismatched sample: CD 21S;  $E_0=10$  keV. The dark area is more relaxed than the bright one.

IV A, Part I), it can be concluded that the dark area is more relaxed than the bright one.

## A. Low-mismatched sample with a large epilayer thickness (CD 21S sample)

### 1. Spectroscopic analysis

Figure 3(a) and Table III show that, at low accelerating beam energy (5 keV), the maximum of luminescence emitted at 300 K from the CD 21S sample occurs at 1.388 eV. By assuming that the CL peak arises at  $E_g(x) + kT/2$ ,<sup>6</sup>  $x$  being the gallium content in the  $\text{Ga}_x\text{In}_{1-x}\text{P}$  epilayer, we find an  $E_g(x=0.055)$  value equal to 1.375 eV. Obviously, this shows that the  $\text{Ga}_x\text{In}_{1-x}\text{P}$  epilayer is not fully relaxed since the band gap of an unstrained  $\text{Ga}_{0.055}\text{In}_{0.945}\text{P}$  epilayer should be equal to 1.391 eV, as calculated with the following relations (Merle *et al.*)<sup>7</sup> which gives the band-gap energy value of an unstrained  $\text{Ga}_x\text{In}_{1-x}\text{P}$  epilayer as a function of its gallium composition  $x$ ;

$$E_g(x) = E_g(0) + 0.77x + 0.684x^2 (x < 0.8), \quad (1)$$

where  $E_g(0)$  is the InP band-gap energy expressed, at temperature  $T$ , by<sup>8</sup>

$$E_g(0) = 1.4539 - 0.0359 \left( 1 + \frac{2}{e^{209/T} - 1} \right). \quad (2)$$

When the accelerating beam energy  $E_0$  increases, but still corresponds to an electron-hole pairs generation within the epilayer alone, the CL peak is redshifted by 13 meV (Table III). As shown in Ref. 2, this is due to the recycling, by the epilayer, of the photons created there. But, on the opposite to what was observed in InP/InP homojunctions,<sup>2</sup> the full width at half maximum (FWHM) of the CL peak increases with  $E_0$  (Table III), whereas, in presence of the photon recycling process described previously, it should decrease.<sup>2,9,10</sup> Furthermore, the 5 keV CL peak extends quite largely toward the low energy part of the spectrum with respect to what is usually obtained in specimens doped at a low level.<sup>2,6</sup> Since, as shown in Ref. 2, the  $n^+$  substrate CL spectrum extends from 1.25–1.55 eV, the unexpected increase of the FWHM with  $E_0$  results from a larger and larger participation, with  $E_0$  of the substrate luminescence to the whole spectrum. The participation of the InP buffer luminescence to the whole CL cannot be excluded, even if its thickness is only one tenth of that of the  $\text{Ga}_x\text{In}_{1-x}\text{P}$  epilayer. But, at 300 K, it cannot be distinguished from the substrate luminescence.

When, at 20 keV, the electron beam starts penetrating the substrate, a large and sudden redshift of 12 meV associated with a large increase of the FWHM of 15 meV is observed (Table III). This shows that the substrate luminescence starts to dominate and the whole CL spectrum becomes widely spread out toward the low-energy side, i.e., for photons with energies smaller than 1.36 eV [Fig. 3(a)]. The high-energy side of the CL spectra presents an inflexion point at 1.388 eV which corresponds to the 5-keV CL peak, i.e., to the  $\text{Ga}_x\text{In}_{1-x}\text{P}$  luminescence.

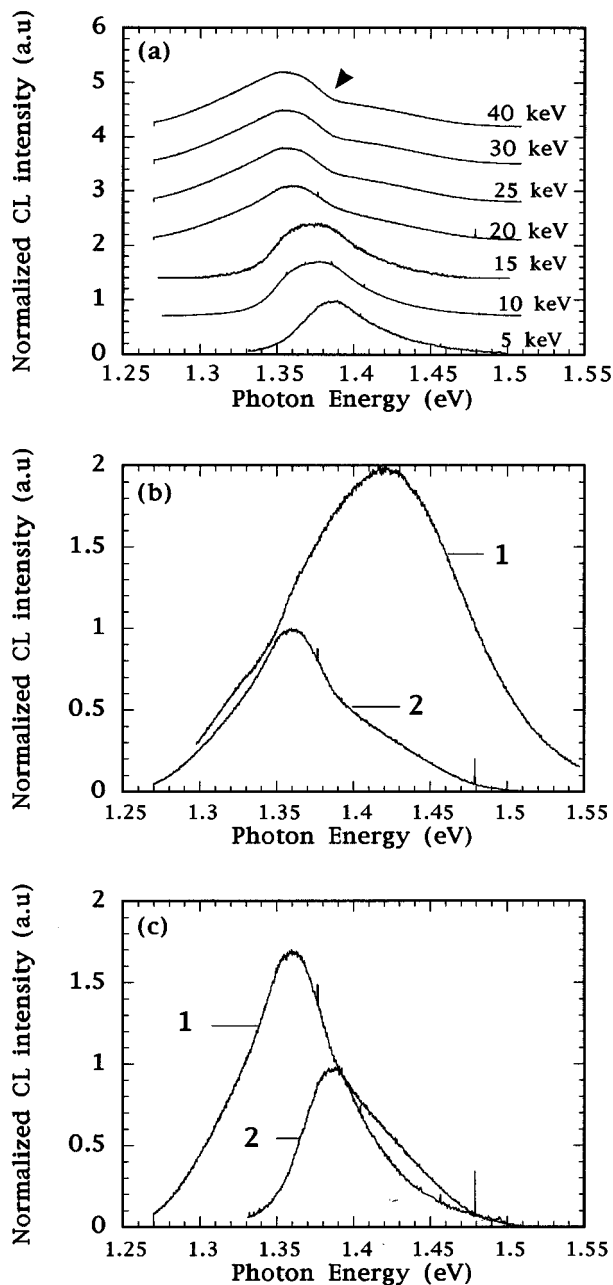


FIG. 3. Low-mismatched sample: CD 21S sample. (a) Evolution, with  $E_0$ , of the 300-K CL spectra recorded on the bright area. When  $E_0$  increases, the CL peak is red-shifted, and the FWHM increases. The peak positions and FWHM are listed in Table III. The arrow indicates the inflexion point. (b) Normalized CL spectra recorded at 300 K showing that the substrate luminescence which is filtered by the  $\text{Ga}_x\text{In}_{1-x}\text{P}$  layer is, at 40 keV, equal to 0.4 times (1/2.5) the total substrate luminescence. Curve 1:  $E_0 = 5$  keV (substrate alone<sup>2</sup>); curve 2:  $E_0 = 20$  keV (CD 21S sample). (c) Normalized CL spectra recorded on the CD 21S Sample at 300 K showing that the CL intensity collected from the substrate exclusively is 1.7 times that collected from the  $\text{Ga}_x\text{In}_{1-x}\text{P}$  epilayer. Curve 1:  $E_0 = 20$  keV; curve 2:  $E_0 = 5$  keV.

At 25 keV and above, the CL peak becomes very asymmetrical, and the relative participation of the  $\text{Ga}_x\text{In}_{1-x}\text{P}$  epilayer to the whole luminescence (at photon energies above 1.355 eV) decreases notably. The position of the CL peak remains constant with  $E_0$  [Fig. 3(a), Table III]. The substrate radiations are mainly filtered by the  $\text{Ga}_x\text{In}_{1-x}\text{P}$  epilayer rather than by the InP buffer since the CL peak arises at

TABLE III. CD 21S sample. Variation, with  $E_0$ , of the 300 K CL peaks and FWHM. The electron penetration depth,  $R_p$  is the Grün<sup>14</sup> range.

$E_0$ (keV)	$R_p$ ( $\mu\text{m}$ )	CL peak position (eV)	FWHM (meV)
5	0.16	1.388	54
10	0.54	1.379	60
15	1.09	1.375	60
20	1.8	1.36	75
25	2.67	1.355	75.5
30	3.67	1.355	
35	4.08	1.355	
40	6.07	1.355	

1.355 eV and not at 1.33 eV as in the case of the InP/InP homojunction.<sup>2</sup> The difference of 20 meV between the CL peak and the band gap of the partially strained  $\text{Ga}_{0.055}\text{In}_{0.945}\text{P}$  layer calculated at 300 K (1.375 eV) shows that the absorption of the substrate radiations by the  $\text{Ga}_x\text{In}_{1-x}\text{P}$  epilayer starts on extrinsic impurity levels in the band gap. The low-energy part of the CL spectra (below 1.355 eV) corresponds to the substrate luminescence alone. The filtering of the substrate radiations by the uppermost epilayer has already been observed in InP/InP homojunctions.<sup>2</sup> Figure 3(b) shows CL curves recorded on the substrate alone (curve 1) and on the CD 21S sample (curve 2). The curves reveal that this filtering is also quite efficient here. As a matter of fact, in presence of the epilayer (CD 21S specimen; curve 2) only 40% of the total, and therefore not filtered, CL intensity is collected.

As in the case of the InP/InP homojunction,<sup>2</sup> the epilayer luminescence observed at high accelerating beam energy comes from the recycling, by the epilayer, of photons issued from the substrate.

Figure 3(c) shows two CL spectra recorded on CD 21S sample at low and medium values of the accelerating beam energy  $E_0$ . A comparison of them shows that the participation, even at low accelerating beam energy (5 keV), of the substrate to the whole luminescence, allows us to assume that the minority carrier diffusion length is approximately equal to the difference between the sum of the  $\text{Ga}_x\text{In}_{1-x}\text{P}$  and InP epilayer thicknesses (Table I) and the 5 keV electron penetration depth (Table III), i.e., 1  $\mu\text{m}$ . In the next paragraph, we determine more precisely this value by means of semi-quantitative CL measurements. The experiments are performed on the bright and dark areas in order to point out any difference in the epilayer diffusion length and/or doping level, and in the interface recombination velocity.

## 2. DR parameters

The results of the 300 K semi-quantitative CL measurements are shown in Fig. 4. The fits of the experimental curves by the theoretical ones permit to establish DR parameters values of the bright and dark areas which are listed in Table IV.

In the case of a  $\text{Ga}_x\text{In}_{1-x}\text{P}/\text{InP}/\text{InP}$  heterojunction, the number of DR parameters which influence the polychromatic  $I_{\text{CL}}$  curves is quite large:

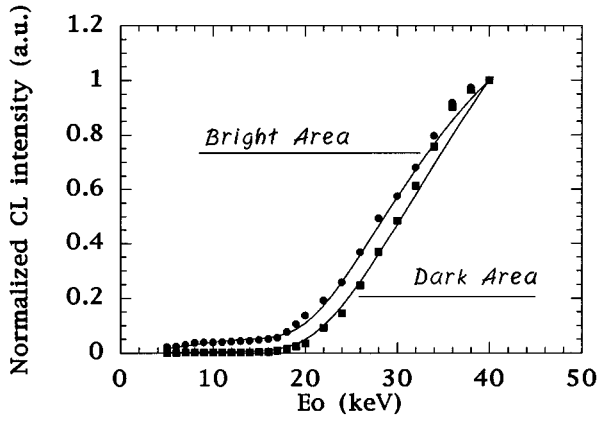


FIG. 4. Polychromatic semi-quantitative CL measurements obtained on the bright and dark areas of the CD 21S sample shown in Fig. 1. Experimental results (●,■) and best fits (—).

- (i) Minority carrier diffusion lengths in the  $\text{Ga}_x\text{In}_{1-x}\text{P}$  and InP epilayers, and in the substrate.
- (ii) Free surface minority carrier recombination velocity.
- (iii)  $\text{Ga}_x\text{In}_{1-x}\text{P}/\text{InP}$  and InP/InP interface minority carrier recombination velocities.
- (iv) Optical absorption coefficients in the two epilayers and in the substrate.

The previous characterization of an  $n^+$ -InP substrate and an  $n\text{-InP}/n^+$  InP homojunction<sup>2</sup> allows us to make different assumptions concerning the value of a few parameters:

- (i) The minority carrier diffusion length in the InP buffer is equal to  $0.7 \mu\text{m}$ , i.e., is larger than the buffer thickness. Therefore, its precise value, which is always larger than the buffer thickness, has no influence on the  $I_{\text{CL}}$  curves.
- (ii) The InP/InP recombination velocity can be as large as  $4 \times 10^5 \text{ cm/s}$ .
- (iii) The optical absorption coefficients in the epilayer and in the substrate are, respectively, taken as  $7000$  and  $50 \text{ cm}^{-1}$ .

The experimental curves are fitted with theoretical curves calculated by means of a diffusion model<sup>2</sup> of which here we will recall the main steps. First, we assume, under beam injection, flat band conditions in the whole structure.<sup>2</sup> Therefore, the stationary excess minority carrier density in

TABLE IV. CD21S sample, 300 K DR parameters of the bright and dark areas.  $L_1$  is the  $\text{Ga}_x\text{In}_{1-x}\text{P}$  diffusion length.  $L_3$  is the substrate diffusion length.  $V_0$  is the free surface recombination velocity.  $V_1$  and  $V_2$  are respectively the  $\text{Ga}_x\text{In}_{1-x}\text{P}/\text{InP}$  and InP/InP recombination velocities.  $M$  is a factor by which the luminescence in the  $\text{Ga}_x\text{In}_{1-x}\text{P}$  epilayer has to be multiplied in order to fit the experimental curves. It accounts for the recycling of substrate photons.

CD 21S sample	$V_0$ (cm/s)	$L_1$ ( $\mu\text{m}$ )	$V_1$ (cm/s)	$V_2$ (cm/s)	$L_3$ ( $\mu\text{m}$ )	$M$
Bright area	$3.10^6$	0.9	$7.10^5$	$3.10^6$	0.6	3200
Dark area	$3.10^6$	0.9	$3.10^6$	$3.10^6$	1.5	320

each layer,  $\Delta p_i(z)$  ( $i=1-3$ ), created by the electron beam in the homogeneous  $n$ - and  $n^+$ -type materials, is given by the one-dimensional continuity equation;

$$D_i \frac{d^2 \Delta p_i(z)}{dz^2} - \frac{\Delta p_i(z)}{\tau_i} = -g(z), \quad (3)$$

where  $D_i$  is the diffusion coefficient in the  $i$ st layer. It is related to the diffusion length  $L_i$  by the relation  $L_i = (D_i \tau_i)^{1/2}$ , where  $\tau_i$  is the excess carrier total lifetime given by  $1/\tau_i = 1/\tau_{nr} + 1/\tau_{ri}$ ;  $\tau_{nr}$  and  $\tau_{ri}$  are, respectively, the nonradiative and the radiative lifetimes.  $g(z)$  is the one-dimensional generation function of electron-hole pairs in the specimen; we have chosen  $g(z)$  given by the analytical function derived by Akamatsu *et al.*<sup>11</sup> from Monte Carlo simulations.  $\Delta p_i(z)$  can be expressed as<sup>2,4</sup>

$$\Delta p_i(z) = C_i^+ \exp(z/L_i) + C_i^- \exp(-z/L_i) + \int_{V/2}^{L_i} \exp\left(-\frac{|z-z'|}{L_i}\right) \frac{g(z')}{D_i} dz', \quad (4)$$

where  $L_i$  is the diffusion length in the  $i$ st layer.

The boundary conditions which allow the determination of the constants  $C_i^+$  and  $C_i^-$  are as follows:

(a) At the free surface located at  $z=0$  ( $i=1$ ;  $\text{Ga}_x\text{In}_{1-x}\text{P}$  epilayer):

$$D_1 \frac{d\Delta p_1(z)}{dz} = V_0 \Delta p_1(z), \quad (5)$$

where  $V_0$  is the free surface recombination velocity (cm/s) of the minority carriers. The first term is the diffusive hole current density  $\mathbf{j}_1$  in the  $\text{Ga}_x\text{In}_{1-x}\text{P}$  epilayer.

(b) At the  $\text{Ga}_x\text{In}_{1-x}\text{P}/\text{InP}$  interface located at  $z=t_1$ :

$$\mathbf{j}_1(t_1) - \mathbf{V}_{12} \Delta p_1(t_1) = \mathbf{j}_2(t_1), \quad (6)$$

$$\mathbf{j}_2(t_1) - \mathbf{V}_{21} \Delta p_2(t_1) = \mathbf{j}_1(t_1), \quad (7)$$

where  $\mathbf{j}_2$  is the diffusive hole current density in the InP buffer.  $\mathbf{V}_{12}$  and  $\mathbf{V}_{21}$  are the recombination velocities of the interface, respectively, on the side of  $\text{Ga}_x\text{In}_{1-x}\text{P}$  and of InP. By taking  $\mathbf{V}_{12}$  equal to  $\mathbf{V}_{21}$  (named  $\mathbf{V}_1$  in the following), one obtains the third boundary condition,

$$\Delta p_1(t_1) = \Delta p_2(t_1). \quad (8)$$

(c) At the InP/InP interface located at  $z=t_2$ :

Similarly to the previous boundaries conditions, we can write:

$$\mathbf{j}_2(t_2) - \mathbf{V}_{23} \Delta p_2(t_2) = \mathbf{j}_3(t_2), \quad (9)$$

$$\mathbf{j}_3(t_2) - \mathbf{V}_{31} \Delta p_3(t_2) = \mathbf{j}_2(t_2), \quad (10)$$

where  $\mathbf{j}_3$  is the diffusive hole current density in the InP substrate.  $\mathbf{V}_{23}$  and  $\mathbf{V}_{31}$  are the recombination velocities of the interface, respectively, on the side of the buffer and of the substrate. The fifth boundary condition is:

$$\Delta p_3(t_2) = \Delta p_2(t_2). \quad (11)$$

(d)  $z$  infinite ( $i=3$ )

$$\Delta p_3(z) = 0. \quad (12)$$

This condition leads to  $C_3^+ = 0$ .

The CL intensity collected from the heterojunction is given by<sup>2</sup>

$$I_{CL} = (1-R) \left( BMn_{(0,1)} \int_0^{t_1} A_1(z) \Delta p_1(z) dz \right. \\ \left. + Bn_{(0,2)} \int_{t_1}^{t_2} A_2(z) \Delta p_2(z) dz \right. \\ \left. + Bn_{(0,3)} \int_{t_2}^{\infty} A_3(z) \Delta p_3(z) dz \right), \quad (13)$$

where  $R$  is the reflection coefficient at the  $\text{Ga}_x\text{In}_{1-x}\text{P}/\text{vacuum}$  interface. Its expression depends on the  $\text{Ga}_x\text{In}_{1-x}\text{P}$  refraction index  $n$ . Due to the low gallium content of the  $\text{Ga}_x\text{In}_{1-x}\text{P}$  epilayer, we approximate  $n$  to 3.6 which is the refraction index of InP. For the same reason, no reflection at the  $\text{Ga}_x\text{In}_{1-x}\text{P}/\text{InP}$  interface has been assumed.  $B$  is the radiative constant which has been assumed identical in each layer.  $n_{(0,1)}$ ,  $n_{(0,2)}$ , and  $n_{(0,3)}$  are the doping levels in respectively, the  $\text{Ga}_x\text{In}_{1-x}\text{P}$  epilayer, the InP buffer and the  $n^+$  substrate. The functions  $A_i(z)$  within the integrals account for the photon optical losses during their travel, within the material, to the free surface. For the  $\text{Ga}_x\text{In}_{1-x}\text{P}$  epilayer, this gives

$$A_1(z) = \int_0^{\theta_c} \exp\left(\frac{-\alpha_1 z}{\cos \theta}\right) \sin \theta d\theta, \quad (14)$$

where  $\alpha_1$  is the optical absorption coefficient in the  $\text{Ga}_x\text{In}_{1-x}\text{P}$  epilayer. We take it equal to  $7000 \text{ cm}^{-1}$ .  $\theta_c$  is the critical angle for total reflection at the internal semiconductor/vacuum surface.

The  $\text{Ga}_x\text{In}_{1-x}\text{P}$  band gap is larger than the InP band gap. This results in the full transmission of the radiations issued from the InP buffer through the  $\text{Ga}_x\text{In}_{1-x}\text{P}$  epilayer;

$$A_2(z) = \int_0^{\theta_c} \exp\left(\frac{-\alpha_2(z-t_1)}{\cos \theta}\right) \sin \theta d\theta, \quad (15)$$

where  $\alpha_2$  is the optical absorption coefficient in the InP buffer. Due to the low gallium content, we take it equal to  $\alpha_1$ .

The substrate is highly doped and, as shown in the last paragraph, its luminescence extends from 1.25–1.55 eV. Thus, the substrate photons are partially absorbed by the InP buffer and by the  $\text{Ga}_x\text{In}_{1-x}\text{P}$  epilayer, such that

$$A_3(z) = \int_0^{\theta_c} \exp\left(\frac{-\alpha'_1 t_1}{\cos \theta}\right) \sin \theta d\theta, \\ \int_0^{\pi} \exp\left(\frac{-\alpha'_2(t_2-t_1)}{\cos \theta}\right) \sin \theta d\theta, \\ \int_0^{\pi} \exp\left(\frac{-\alpha_3(z-t_2)}{\cos \theta}\right) \sin \theta d\theta. \quad (16)$$

$\alpha'_1$ ,  $\alpha'_2$ , and  $\alpha_3$  are the optical absorption coefficients of photons issued from the substrate and absorbed, respectively, by the  $\text{Ga}_x\text{In}_{1-x}\text{P}$  epilayer, the InP buffer and by the substrate itself. In Eq. (13) of the CL intensity, the factor  $M$  accounts for the absorption of substrate photons by the  $\text{Ga}_x\text{In}_{1-x}\text{P}$  epilayer. As a matter of fact, such an absorption creates electron-hole pairs which, in turn, create extra

photons.<sup>2</sup> As it was already shown in Fig. 3(b), 40% of the total number of photons created within the substrate can reach the free surface without being absorbed by the two epilayers. The absorption within the InP buffer is considered as negligible since no luminescence associated to it could be really detected, in agreement with the small thickness of this layer. As stated previously,<sup>2</sup>  $\alpha_3$  is taken equal to  $50 \text{ cm}^{-1}$ .<sup>12</sup> By recalling that we deal with the modeling of the external luminescence, and that only the substrate radiations with an energy smaller than 1.33 eV leave the heterostructures, we set to zero the absorption coefficients  $\alpha'_1$  and  $\alpha'_2$ . The absorption, by the  $\text{Ga}_x\text{In}_{1-x}\text{P}$  epilayer, of the photons issued from the substrate is described by the prefactor  $M$  of Eq. (13).

The polychromatic  $I_{CL}$  curves are calculated, for the bright area, under drastic conditions that we summarize below, and which result from our previous analysis of the 300 K CL spectra:

- (i) At 5 and 10 keV, the CL intensity from the  $\text{Ga}_x\text{In}_{1-x}\text{P}/\text{InP}/\text{InP}$  structure comes from the  $\text{Ga}_x\text{In}_{1-x}\text{P}$  epilayer alone [Fig. 3(a)].
- (ii) At 20 keV, the luminescence from the substrate is equal to 1.7 times that from the epilayer [Fig. 3(c)].
- (iii) At accelerating beam energies higher than 25 keV, the CL intensity from the  $\text{Ga}_x\text{In}_{1-x}\text{P}/\text{InP}/\text{InP}$  structure is issued from the substrate alone [Fig. 3(a)].
- (iv) 40% of the total substrate intensity is collected [Fig. 3(b)].

In the absence of any 300-K CL spectra of the dark area, we assume, in the light of the CL intensities listed in Table II, that (i) the  $\text{Ga}_x\text{In}_{1-x}\text{P}$  CL intensity ( $I_{CL1}$ ) in the dark area is, at 5, 10, and 15 keV, 10% of the bright area intensity and (ii) the substrate intensity ( $I_{CL3}$ ) in the dark area is 0.98 times that in the bright area.

The DR parameters which give the best fits of the experimental curves obtained on the bright and dark areas are listed in Table IV. The value of the free surface recombination velocity,  $3 \times 10^6 \text{ cm/s}$ , seems quite large for an InP-based material.<sup>13</sup> This could be explained by the presence of a residual electric field in the epilayer due to the large doping level difference between the epilayer and the substrate. This could also result from the presence of many recombination centers at the surface.

The InP/InP recombination velocity, equal to  $3 \times 10^6 \text{ cm/s}$ , is area independent. Its very large value, as compared to that previously determined in InP/InP homojunctions,<sup>2</sup> could be due to slight differences in the elaboration conditions.

The value of the diffusion length  $L_1$  ( $=0.9 \mu\text{m}$ ) in the  $\text{Ga}_x\text{In}_{1-x}\text{P}$  epilayer is close to that previously determined by spectroscopic measurements. This shows that, similarly to what is usually observed in undoped semiconductors, the electron-hole pairs recombination is of the Shockley–Read–Hall type, i.e., is dominated by deep levels. By assuming a doping level of  $3 \times 10^{14} \text{ cm}^{-3}$  in the epilayer, one can estimate the luminescence efficiency equal to 1%. An area-

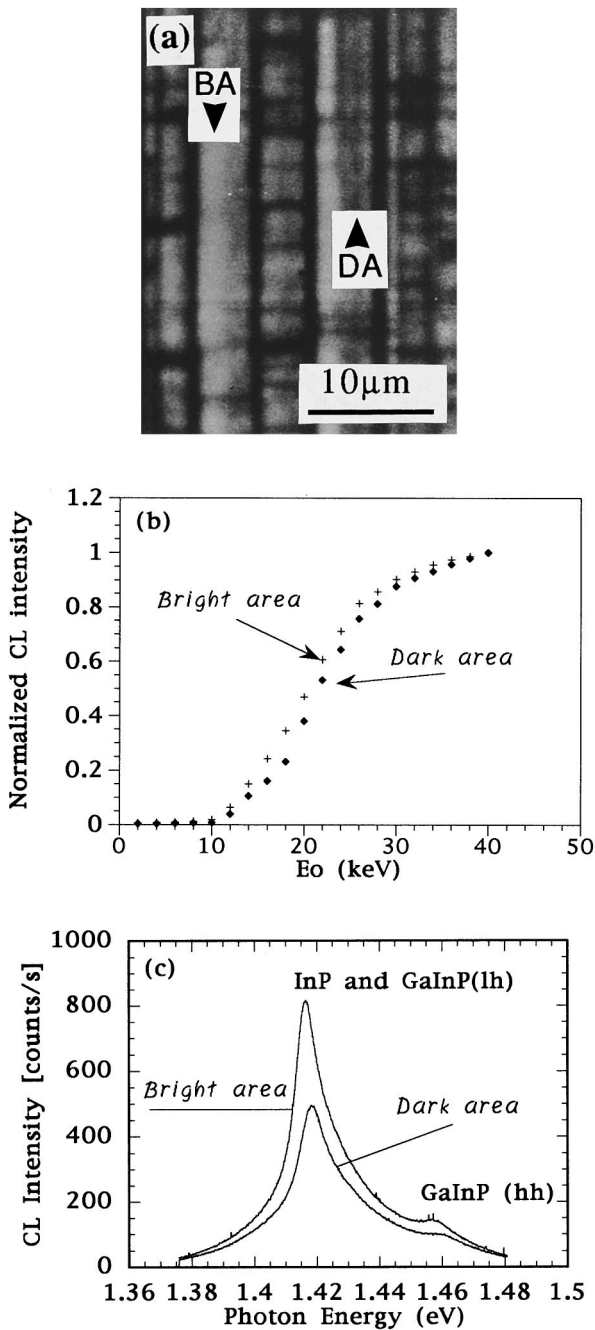


FIG. 5. Low-mismatched sample: CF 86S ( $x_{\text{Ga}}=7.8\%$ ;  $\Delta a/a=0.56\%$ ;  $R[1\bar{1}0]=3.6\%$ ;  $R[110]=12.9\%$ ). (a) Plan-view polychromatic CL image. (b) Variation, with the accelerating beam energy, of the polychromatic CL intensity recorded at 300 K on the same bright and dark areas as in (c). (c) Typical 77-K CL spectra recorded at 5 keV on a bright and dark area. The dark area is more relaxed than the bright one.

independent diffusion length seems quite contradictory with the fact that the bright area luminescence is 10 times higher than the dark area luminescence.

But first, it should be recalled that the DR parameters in both areas have been deduced from the shape of the normalized curves [Fig. 3(a)], which have been both calculated for an identical doping level ratio of 33 000 ( $1 \times 10^{19}/3 \times 10^{14}$ ) between the substrate and the epilayer. Second, when comparing the values of the CL intensities calculated at 40 keV and corresponding to the sets of DR parameters listed in

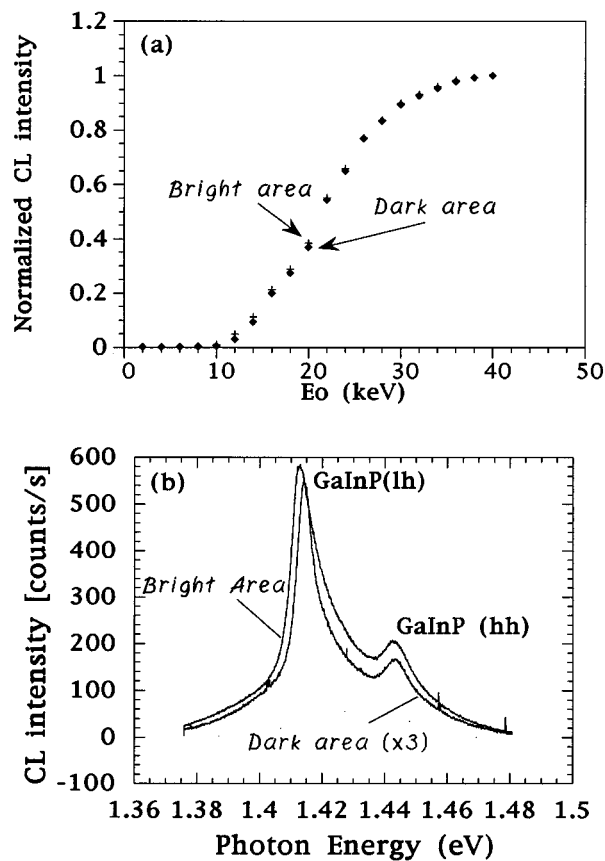


FIG. 6. Low-mismatched sample: CE 88S ( $x_{\text{Ga}}=6.5\%$ ;  $\Delta a/a=0.47\%$ ;  $R[1\bar{1}0]=1.5\%$ ;  $R[110]=1.5\%$ ). (a) Variation, with the accelerating beam energy, of the polychromatic CL intensity recorded at 300 K on the same bright and dark areas as in (b). (b) Typical 77 K CL spectra recorded at 5 keV on a bright and dark area. The dark area is more relaxed than the bright one.

Table IV, we find that the CL intensity in the dark area should be 5 times larger than that in the bright area. Since we have found experimentally that both areas have the same CL intensity at 40 keV (Table II), and remembering that the CL intensity is proportional to the doping level as shown in Eq. (13), it can be reasonably deduced that the doping level in the substrate part of the dark area is 5 times lower than that

TABLE V. CF 86S sample. Variation, with  $E_0$ , of the polychromatic CL intensity recorded at 300 K on the bright and dark areas. This table shows that the large CL intensity difference between the two areas is observed at low keV.

$E_0$ (keV)	CL intensity (a.u.) bright area	CL intensity (a.u.) dark area
2	2	0.8
4	2.8	1
6	3.2	1.3
8	4.1	1.9
10	6	2.8
12	21.8	13.4
14	51.2	35.7
16	82.4	54.3
18	117.5	77.9

TABLE VI. CF 88S sample. Variation, with  $E_0$ , of the polychromatic CL intensity recorded at 300 K on the bright and dark areas. Same comment as in Table V.

$E_0$ (keV)	CL intensity (a.u.) bright area	CL intensity (a.u.) dark area
2	0.5	0.3
4	0.7	0.5
6	1	0.8
8	1.3	1
10	3	1.8
12	14.7	9.2
14	33.3	27.8
16	63.5	59.2
18	86.2	81.5

in the substrate part of the bright area. This is in agreement with the larger diffusion length  $L_3$  found in the dark area. As a matter of fact, a lower doping level in the substrate part of the dark area could lead to a recombination of the SRH type, and to a diffusion length of the order of  $1 \mu\text{m}$  as experimentally observed. Concerning the substrate part of the bright area, the recombination of carriers could be of the radiative type, as a result of a lower density of nonradiative recombination centers. The last conclusion of the comparison between experimental and calculated CL intensities is that the epilayer part of the dark area is less doped than the epilayer part of the bright area. The substrate to epilayer doping levels ratio is constant. The diffusion length does remain constant in the epilayer since, at such a low doping level, the recombination is always of the SRH type.

The value of the substrate diffusion length  $L_3$  influences the slope of the  $I_{\text{CL}}$  curves at high accelerating beam energies only (here above 20 keV). Therefore, as we have seen previously, the different values of  $L_3$  found in the bright and dark areas are not responsible for the large CL contrast experimentally observed. The data in Table IV show that this contrast comes first from the difference of the  $\text{Ga}_x\text{In}_{1-x}\text{P}/\text{InP}$  recombination velocities. Thus, the higher value of the recombination velocity in the dark area (Table IV) can be related to a higher density of misfit dislocations at the  $\text{Ga}_x\text{In}_{1-x}\text{P}/\text{InP}$  interface such those analyzed by plan-view TEM (see Part I of this paper). This confirms the spectroscopic results which showed a lower strain in the dark than in the bright area (Fig. 2).

TABLE VII. CE 84S sample. Variation, with  $E_0$ , of the polychromatic CL intensity recorded at 300 K on the bright and dark areas. Same comment as in Table V.

$E_0$ (keV)	CL intensity (a.u.) bright area	CL intensity (a.u.) dark area
6	1.1	0.5
10	17.2	12.5
12	39.6	30.2
14	93.2	68.2
16	158.2	129
18	209.1	162

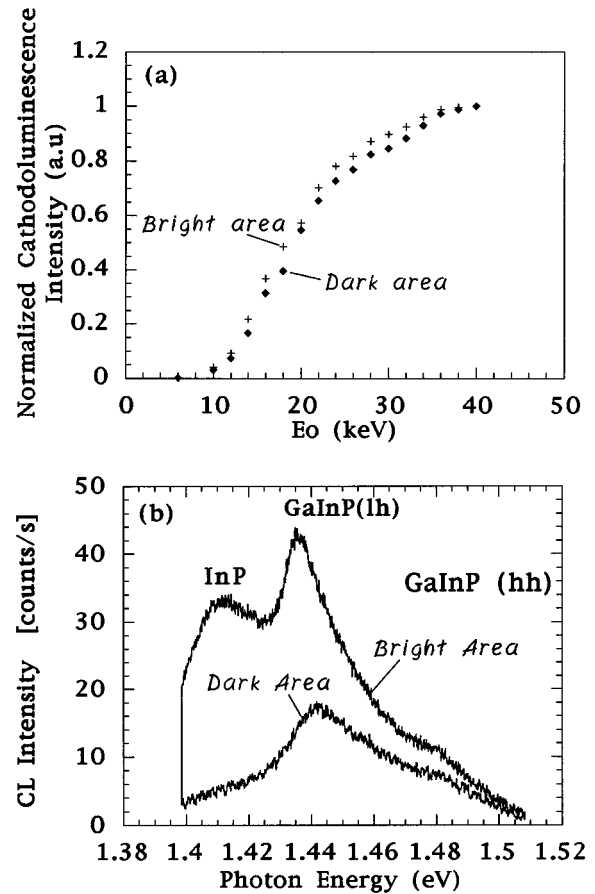


FIG. 7. Highly mismatched sample: CE 84S ( $x_{\text{Ga}}=11.2\%$ ;  $\Delta a/a=0.80\%$ ;  $R[1\bar{1}0]=13\%$ ;  $R[110]=43\%$ ). (a) Variation, with beam energy, of the polychromatic CL intensity recorded at 300 K on the same bright and dark areas as in (b). (b) Typical 77 K CL spectra recorded at 5 keV on a bright and dark area. The dark area is more relaxed than the bright one.

Finally, the CL contrast of the two areas is most influenced by the value of the factor  $M$  by which the  $\text{Ga}_x\text{In}_{1-x}\text{P}$  luminescence ( $I_{\text{CL}1}$ ) has to be multiplied in order to fit the  $I_{\text{CL}}$  curves.<sup>2</sup> As stated previously, the factor  $M$  comes from the recycling, by the epilayer, of the photons issued from the substrate and absorbed by it,<sup>2</sup> in agreement with our analysis of the spectroscopic results. We find that the value of  $M$  is much higher in the bright ( $M=3200$ ) than in the dark area ( $M=320$ ). This difference can have three origins. The first comes from the fact that the epilayer part of the bright area has a smaller energy band gap. This induces a higher absorption, by the epilayer, of the photons issued from the substrate. The second comes from a higher production of photons by the substrate part of the bright area due to its higher doping level. The third comes from the fact that, the smaller the  $\text{Ga}_x\text{In}_{1-x}\text{P}/\text{InP}$  recombination velocity, the larger the number of photons created in the substrate, at low keV, by diffusion of holes from the epilayer.

The luminescence heterogeneity such as that described previously, has not been currently observed in the specimens we have studied. But, as it has been shown, it results mainly from local variations of the doping level, and also from different  $\text{Ga}_x\text{In}_{1-x}\text{P}/\text{InP}$  recombination velocities.



## B. Analysis of the other samples

One important result of the analysis presented in the last paragraph is that the minority carrier diffusion length in the epilayer  $L_1$  is area independent. Furthermore, its value (0.9  $\mu\text{m}$ ) is larger than the epilayer thickness (0.44–0.55  $\mu\text{m}$ ) of the three other specimens we have studied. Therefore, it can be assumed with great confidence that, in these three samples, the excess carriers created within the epilayer diffuse toward the substrate where they recombine.

The CL plan-view image in Fig. 5(a) is an example of dark and bright areas which have been selected for spectroscopic and semi-quantitative CL analysis. The results obtained on two low-mismatched samples (CF 88S and CF 86S, see Table I) are put together in Figs. 5 and 6. These figures point out that the CL intensity recorded at low accelerating beam energy is much lower on dark than on bright areas [Figs. 5(b) and 6(a)]. Tables V and VI which display the values of the CL intensity in both samples, indicate that the CL contrast between dark and bright areas is much more pronounced at low than at high accelerating beam energy. Therefore, the luminescence heterogeneities are connected with fluctuations at the  $\text{Ga}_x\text{In}_{1-x}\text{P}/\text{InP}$  interface and not in the InP substrate. Furthermore, the epilayer luminescence observed at low accelerating beam energy is due to the recycling of the photons emitted by the substrate, the carriers created inside the epilayer by the electron beam diffuse toward the InP substrate. This suggests that the  $\text{Ga}_x\text{In}_{1-x}\text{P}/\text{InP}$  interface recombination velocity should be higher in the case of dark areas. The CL peaks associated to the CB-lh and CB-hh transitions occurs at a higher energetical position in the case of dark areas [Fig. 5(c) and 6(b)]. This last result points out their higher relaxation rate, in agreement with a higher value of their interface recombination velocity.

Tables VII and Figs. 7(a) and 7(b) show similar results which have been obtained on a highly mismatched sample. The same variations as those noticed previously, between bright and dark areas are easily seen from semi-quantitative [Fig. 7(a)] and spectroscopic [Fig. 7(b)] CL curves. When the relaxation becomes quite large, the InP buffer peak can disappear [Fig. 7(b)]. This can be correlated with the results

obtained by means of transmission electron microscopy experiments where dislocations running through the buffer could be observed.<sup>1</sup>

## IV. CONCLUSION

We have demonstrated, by associating semi-quantitative and spectroscopic CL studies, that the spatial variations of the luminescence in tensile strained  $\text{Ga}_x\text{In}_{1-x}\text{P}/\text{InP}/n^+\text{-InP}$  heterostructures was due to spatial variations of the dislocations located at the  $\text{Ga}_x\text{In}_{1-x}\text{P}/\text{InP}$  interface. We have also shown that these luminescence fluctuations are greatly enhanced in the case of a highly doped substrate, as a result of photon recycling.

## ACKNOWLEDGMENTS

H. Mariette (CNRS/CENG, Grenoble) is greatly acknowledged for valuable discussions.

- <sup>1</sup>F. Cléton, B. Sieber, A. Lefebvre, A. Bensaada, R. A. Masut, J. M. Bonard, J. D. Ganière, and M. Ambri, *J. Appl. Phys.* **80**, 827 (1996).
- <sup>2</sup>F. Cléton, B. Sieber, L. Isnard, R. A. Masut, J. M. Bonard, and J. D. Ganière, *Semicond. Sci. Technol.* **11**, 726 (1996).
- <sup>3</sup>A. Bensaada, A. Chennouf, R. W. Cochrane, R. Leonelli, P. Cova, and R. A. Masut, *J. Appl. Phys.* **71**, 1737 (1992); A. Bensaada, R. W. Cochrane, R. A. Masut, R. Leonelli, and G. Kajrys, *J. Cryst. Growth* **130**, 433 (1993).
- <sup>4</sup>C. De Meerschman, B. Sieber, J. L. Farvacque, and Y. Druelle, *Microscop. Microanal. Microstruc.* **3**, 486 (1992).
- <sup>5</sup>G. E. Pikus and G. L. Bir, *Sov. Phys. Solid State* **1**, 136 (1959).
- <sup>6</sup>H. B. Bebb and E. W. Williams, in *Semiconductors and Semimetals*, edited by R. K. Willardson and A. C. Beer (Academic, New York, 1972); Vol. 8.
- <sup>7</sup>P. Merle, D. Auvergne, H. Mathieu, and J. Chevallier, *Phys. Rev. B* **15**, 2032 (1977).
- <sup>8</sup>L. Pavesi, F. Piaaza, A. Rudra, J. F. Carlin, and M. Ilegems, *Phys. Rev. B* **44**, 9052 (1991).
- <sup>9</sup>R. K. Ahrenkiel, D. J. Dunlavy, and T. J. Hanak, *J. Appl. Phys.* **64**, 1916 (1988).
- <sup>10</sup>R. K. Ahrenkiel, B. M. Keyes, and D. J. Dunlavy, *Sol. Cells* **30**, 163 (1991).
- <sup>11</sup>B. Akamatsu, J. Henoc, and P. Henoc, *J. Appl. Phys.* **52**, 7245 (1981).
- <sup>12</sup>M. Bugajski and W. Lewandowski, *J. Appl. Phys.* **57**, 521 (1985).
- <sup>13</sup>R. K. Ahrenkiel, *Properties of Indium Phosphide* (INSPEC, London, 1991), p. 80.
- <sup>14</sup>A. E. Grün, *Z. Naturforsch.* **12a**, 89 (1957).